Response to reviewer comments

We would like to thank the reviewer for their thorough evaluation of our manuscript and for the constructive comments and suggestions. We have carefully revised the manuscript according to the comments. In the following, we provide a detailed, point-by-point response to all the comments. For clarity, the comments are presented in italics, followed by our responses. All changes made in the manuscript are highlighted in the revised version.

Potential issues with the model description

- 1) Model description does not seem to match implementation:
- a. Lines 126 127: "SLDOC degradation is driven primarily by photodegradation" this contrasts against the equation on line 215 stating it is only a function of τ !". The photodegradation option (bg_ctrl_bio_remin_RDOM_photolysis) in the model configuration file provided is commented out and defaults to off (false) in the definition.xml file.

Response:

After carefully re-checking the model configuration files, we realized that original description was inaccurate. In our simulations, the photodegradation option (bg_ctrl_bio_remin_RDOM_photolysis) is indeed commented out in the configuration file and defaults to "false" in the definition.xml. Therefore, SLDOC degradation is not driven by photodegradation in the current model setup. Instead, it is represented by a prescribed lifetime (τ) , as shown in the equation on Line 210. Accordingly, we have revised the sentence in **Lines 129-130** to: "LDOC degradation is temperature dependent, SLDOC degradation is represented by a prescribed lifetime (τ) , and a fraction of SLDOC is converted into RDOC."

b. The gas transfer velocity equation does not match that in Ridgwell et al., (2007) as stated. Parameters l, a, b, c and the 0.25 do not appear in that paper or in genie's piston velocity code. This may be referring to combined processes in the model but I cannot find the a, b, c and 0.25 parameters in the code. The value for the scaling factor "I" has a value of 2.778e-6 which seems like the preindustrial molar ratio of CO₂ in the atmosphere but I cannot see how this relates to gas transfer velocity specifically.

Response:

The parameters l, a, b, c, and 0.25 do not appear in Ridgwell et al. (2007). These terms were originally taken from Ridgwell (2001), and we mistakenly attributed them to the latter. To avoid confusion, we have revised the manuscript to present the standard formulation of the air-sea CO₂ gas transfer velocity following Wanninkhof (1992), which is consistent with the cGENIE model implementation. The corrected description is now given in the Supporting Information (Section 1). In the revised text, we now clearly state that: 'CO₂ solubility and the Schmidt number are parameterized following

Wanninkhof (1992); The gas transfer velocity k follows the standard quadratic windspeed dependence with a scaling factor of 0.31.' To improve clarity and avoid over complicating the main text, the detailed formulation and parameter definitions have now been moved to the Supporting Information. The unnecessary parameters that caused confusion have been removed.

c. Line 159: "Eppley's initial values, with a = 0.59 and b = 75.80"-the model default value for b (par_bio_kT_eT) is 15.8. These values appear unchanged in the model configuration file or elsewhere in the code, so I can't see how 75.80 is arrived at.

Response:

In the cGENIE configuration and code, the default value is b = 15.8 (parameter par_bio_kT_eT), which is the value actually used in our simulations. We have corrected the manuscript accordingly (**Line 145**), and now state: "The temperature dependence of biological processes follows Eppley's formulation, with a = 0.59 and b = 15.8." This correction does not affect the simulations or results presented in the paper.

d. Lines 169-173: "v=0.66"-the configuration file has selected the Dunne et al., (2005) option for the particle export ratio (bg_opt_bio_red_DOMfrac='dunne') which is an empirical function dependent on temperature, productivity and euphotic zone depth. This looks like it overrides the default global constant value for v of 0.66, instead creating a spatially variable ratio of particle export to total export (see loc_rPOC on line 991 in biogem_box.f90) from which v (ratio of DOC production to total: 1-locrPOC) is calculated. The Dunne et al., (2005) scheme is also described in the manuscript.

Response:

The original text stated a fixed value of v=0.66, corresponding to the default OCMIP-2 setting in cGENIE (Ridgwell et al., 2007). In our experiments, we employed the Dunne et al. (2005) scheme (bg_opt_bio_red_DOMfrac='dunne'), in which v is dynamically calculated as v = 1 - rPOC, rPOC is an empirical function of temperature (T), where rPOC = 0.419 + 0.0582 ln(PP/Zeu)-0.0101T, bounded between 0.04 and 0.72. We have revised the manuscript (**Lines 161-163**) to clarify this, and the corrected description now explicitly states that v is spatially variable rather than constant. This modification ensures consistency between the model description and the actual implementation.

e. "While some POC sinks to the bottom waters and is eventually buried in sediments, a substantial fraction is remineralized within the water column." – this model has no sediment module enabled and therefore has a reflective sediment boundary where all POC hitting the seafloor is remineralised in the overlying grid-box (see Ridgwell et

Response:

We thank the reviewer for pointing out this important clarification. The original sentence was misleading because the sediment module was not enabled in our model configuration. In our simulations, POC reaching the seafloor is indeed remineralized in the bottom water grid box, following the reflective sediment boundary condition of cGENIE (Ridgwell et al., 2007), and not buried in sediments. Accordingly, we have revised the text to read: "POC sinks to deep water and is remineralized within the water column, returing carbon to the overlying bottom water grid box." (Lines 191-192)

f. Table 1:

- i. Scaling factor "l" does not obviously appear in Crichton et al., (2021) as described here.
- ii. The half saturation constant values do not seem to match those selected in the configuration file (bg_par_bio_c0_PO₄=0.1E-6 and bg_par_bio_c0_Fe=0.10E-09 for PO_4 and Fe respectively). I'm not sure of the relevance to the Crichton or Matsumoto references here either.
- iii. v: see comment d above, the configuration file appears to choose a spatially variable scheme not a global fixed value.

Response:

We revised **Table 1** and removed the entries for the scaling factor "l" and the DOC fraction "v" as suggested in earlier comments. We also acknowledge that in the originally submitted manuscript, the half-saturation constants for PO₄ and Fe listed in Table 1 did not match those used in the model configuration file. In the revised manuscript, the half-saturation constants now match the configuration file values (bg_par_bio_c0_PO₄ = 0.1E-6 and bg_par_bio_c0_Fe = 0.10E-09). These parameter values are directly inherited from the default cGENIE setup.

g. Figure 11: From the equations for LDOC, SLDOC and RDOC production, these are produced in a globally constant ratio of 0.9599:0.04:0.0001. This is also hard-coded in lines 997–999 in biogem_box.f90. Therefore, I would expect the LDOC and SLDOC panels at least to have the same spatial variability but scaled in magnitude. I'm also unsure from the text if the RDOC panel includes production from the SLDOC remineralization.

Response:

The initial partitioning of DOC production among LDOC, SLDOC, and RDOC is set by fixed fractions (0.9599:0.04:0.0001) in the source code (in biogem box.f90).

Consequently, their surface production patterns are indeed spatially similar. However, the subsequent spatial distributions of LDOC, SLDOC, and RDOC diverge substantially due to their distinct remineralization rates and transformation pathways. Specifically, LDOC is highly labile and rapidly remineralized within the surface and upper thermocline, leading to strong surface gradients and minimal penetration depth. In contrast, SLDOC has a longer lifetime, allowing it to be advected and mixed to intermediate and deep waters before remineralization. As a result, SLDOC exhibits a broader and smoother spatial pattern. For RDOC, the field shown in Fig. 5 includes both the small fraction directly produced at the surface (0.01% of total DOC production) and the additional RDOC generated from SLDOC remineralization through the MCP transformation term (a×[SLDOC]). This source introduces a distributed production pathway throughout the water column, particularly in regions of active remineralization, and is responsible for the gradual accumulation and redistribution of RDOC by ocean circulation. Because of its very long lifetime (16000 years), RDOC becomes nearly homogeneous at the global scale, consistent with its weak spatial variability in the figure. Thus, while surface production ratios are fixed, the emergent global DOC distributions reflect the combined effects of distinct decay constants, transformation coupling (parameter a), and advective-diffusive transport, rather than simple proportional scaling of the initial production fields.

h. There is no information on the spin-up protocol. The readme provided suggests the model is spun-up for 30k years from initial conditions. If true, this doesn't seem like sufficient time for RDOC to reach steady-state given its lifetime of 16k years.

Response:

We restarted the model for further 70k years and plot the curve of global mean RDOC concentration with time (the figure below). RDOC concentration almost reach the steady state after the 60,000th year. Therefore, we added the information of mode spin-up in **Lines 114-115**: "The model was run for 100.000 years to reach a steady state, and the result of the last year was used for analysis." The README file has been updated accordingly.

Surface RDOC 52.20 51.20 50.20 649.20 547.20 5447.20 5447.20 5447.20 644.20 642.20 6544.20 6542.20 65

The global mean RDOC concentration with model time.

2) Model description of new developments is ambiguous and/or incomplete: a. POC remineralization should have a sinking rate described.

Response:

In the cGENIE-MCP configuration used in this study, POC remineralization is associated with an explicit sinking velocity that controls the vertical transport and depth-dependent decay of particulate organic carbon. We have now clarified this in **Section 2.2.3**. The revised text now reads (**Lines192-194**): "POC is transported vertically with a prescribed sinking velocity of 125 m day⁻¹ and is remineralized following an exponential attenuation with depth, governed by the characteristic remineralization length scales (POC1 = 589.9 m, POC2 = 1×10^6 m)." These parameters have been included in Table 1 of the revised version for transparency.

b. SLDOC and RDOC remineralization rates (k) are described as temperature-dependent yet the equations state that $k = 1/\tau$. $1/\tau$ also seems to be applied in the model code.

Response:

We have clarified in Line 209. In the present simulations, SLDOC and RDOC remineralization rates are implemented as $k=1/\tau$, with τ being a globally constant value. Although the code provides an option for temperature-dependent remineralization, this feature was not activated in our configuration. The text has been updated to accurately reflect the model implementation. Future work could explore the impact of implementing temperature-dependent remineralization rates on DOC cycling and distribution.

c. The transformation of SLDOC to RDOC is unclear as to whether the SLDOC is transformed to a RDOC remineralization flux or to the RDOC tracer. I think the latter is the case from the code but the naming of flux terms is ambiguous.

Response:

Indeed, the transformation from SLDOC to RDOC in our model refers to the conversion between tracers, rather than to a remineralization flux. Specifically, during the organic matter cycling, a fraction of POM degradation is allocated to different DOC tracers (LDOC, SLDOC, and RDOC) through the variables loc_bio_red_DOMfrac, loc_bio_red_RDOMfrac, and loc_bio_red_URDOMfrac. In the subsequent remineralization process, the SLDOC pool can be partly remineralized to inorganic constituents or further transferred into the RDOC tracer. Therefore, the naming of "flux" in the code refers to the mass transfer between tracers, not to remineralization fluxes in the strict sense. To clarify this mechanism, we have revised the text as: "a is a dimensionless conversion coefficient that represents the transformation of SLDOC into RDOC, following the parameterization of Wang et al. (2023). The resulting RDOC tracer undergoes slow remineralization independently." (Lines 220-222).

d. Ideally there should be differential equations for LDOC, SLDOC and RDOC to fully describe the new DOC cycling in the model.

Response:

In our model, the cycling of DOC pools (LDOC, SLDOC, and RDOC) is already represented through production, remineralization, and transformation fluxes. To clarify the dynamic relationships among these components, we have added the corresponding differential equations in **Section 2.2.2** to explicitly show how DOC concentrations evolve over time:

$$\begin{split} \frac{\partial [LDOC]}{\partial t} &= F_{prod} \cdot f_1 - k_{zLDOC}[LDOC] \\ \frac{\partial [SLDOC]}{\partial t} &= F_{prod} \cdot f_2 - k_{zSLDOC}[SLDOC] - a \left[SLDOC\right] \\ \frac{\partial [RDOC]}{\partial t} &= F_{prod} \cdot (1 - f_1 - f_2) + a \left[SLDOC\right] - k_{zRDOC}[RDOC] \end{split}$$

where F_{prod} is the total net export production of organic carbon. f_1 =0.9599 and f_2 =0.04 are the export partitioning coefficients for LDOP and SLDOP, respectively, based on Wang et al. (2023), k_{zLDOC} is the temperature-dependent remineralization rate of LDOC at z layer; k_{zSLDOC} is the temperature-dependent remineralization rate of SLDOC at z layer (yr⁻¹); k_{zRDOC} is the remineralization rate of RDOC at z layer (yr⁻¹); a is dimensionless conversion coefficient that converts SLDOC into RDOC, which is based on the Wang et al. (2023); SLDOC is converted to RDOC tracer, which then undergoes slow remineralization independently. (Lines 224-229)

e. The degradation rate constant for resolving temperature-dependent DOC (par_bio_remin_DOC_K1) has been changed from the value in Crichton et al., (2021). This should be included in Table 1.

Response:

We have updated Table 1 to include the modified value of par_bio_remin_DOC_K1, with a note indicating that it is adjusted from Crichton et al. (2021) to reflect the temperature-dependent DOC remineralization in our model.

Significance of MCP model development

A key feature of this model is the transformation of SLDOC to RDOC via parameter a, which distinguishes it as a representation of the Microbial Carbon Pump vs. other models of DOC cycling where different pools are unconnected (e.g., MESMO3). The manuscript presents the validation of DOC against observations, but the deep [(R)DOC] can be reproduced by very different models (Lennartz et al., 2024 vs. Hansell et al., 2012). This is because rates of RDOC cycling are smaller than circulation rates leading to a near-uniform distribution, such that the key constraint is the inventory which primarily constrains the magnitude of global fluxes in and out. To demonstrate this is a novel development, what new dynamics does cGENIE-MCP resolve?

One way to demonstrate this would be to show parallel results from the model when a=0. For example, it would be illustrative to see what happens to the DOC inventory across a range of perturbations with a=0.015 and a=0. This could be different atmospheric CO_2 values, differences in the DOC production or lifetimes, or differences in total production.

My concern is that the implementation of the MCP isn't significantly different to previous models. To illustrate this, I've used a steady-state analysis (see below). The production of RDOC in other models (Fin_{RDOC}^{fix}) is typically a fixed fraction of total DOC production:

$$Fin_{RDOC}^{fix} = \Gamma * v * f_{RDOC} \tag{1}$$

where f_{RDOC} is the fraction of RDOC production (e.g., equivalent to 1-f1-f2 in this manuscript) and the parameters follow those in this manuscript. For clarity I have treated this as already integrated over the surface layer, e.g., units of Pg C and Pg C yr¹. In the cGENIE-MCP model the production of RDOC has an additional term reflecting the production arising from SLDOC remineralization:

$$Fin_{RDOC}^{MCP} = \Gamma * v * f_3 + a * \frac{SLDOC}{\tau_{SL}}$$
 (2)

Assuming steady-state, equation (2) can be rewritten in a comparable form to eqn (1):

$$Fin^{MCP}_{RDOC} = \Gamma * \upsilon * (f_3 + a * f_2)$$

where f_2 is the fraction of SLDOC production from total DOC production. If production and the lifetime of RDOC are similar between models then $f_{RDOC} = (f3 + a * f_2)$ to achieve the modern inventory of RDOC at steady-state. In cGENIE-MCP the parameters f_2 , f_3 , a and v are fixed values (note the question about v above however). As such, the two different models (equations (1) and (3)) can be seen to have similar steady-state dynamics where the dynamic term is export production (Γ) which is scaled by a fixed fraction. The steady-state constraint (eqn 6) also implies that RDOC may not be sensitive to a change in τ_{SLDOC} .

This is a simple analysis which doesn't account for different nutrient feedbacks between SLDOC and RDOC cycling but hopefully it encourages the authors to demonstrate that their model behaves in a novel way to other models. What happens if you have a change in SLDOC production or remineralization? Do the models behave differently for the same change in atmospheric CO_2 ? If this has a notable effect on RDOC, which would not be the case in previous models, then this model would be a significant advancement in resolving DOC dynamics.

Response:

We agree that under strict steady-state assumptions, the expression $Fin_{RDOC}^{MCP} = \Gamma * v * (f_3 + a * f_2)$ appears algebraically similar to a fixed-fraction parameterization. However, as the reviewer also notes, the key distinction of the MCP formulation lies in its coupling between DOC pools, rather than in a steady-state balance.

The cGENIE-MCP model introduces a coupling between SLDOC and RDOC through the parameter a, which fundamentally alters the accumulation behavior of the DOC system.

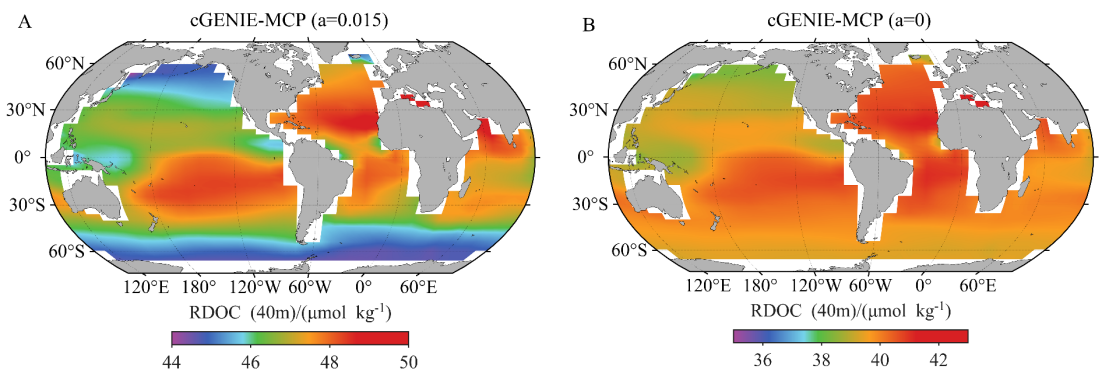
In previous models (e.g., MESMO3: DOC is only divided into two types, namely DOC and RDOC.), DOC and RDOC pools are independent, and the deep DOC inventory depends solely on surface production and a fixed remineralization rate. In contrast, the MCP formulation allows part of the SLDOC to be transformed into RDOC continuously throughout the water column. This introduces a feedback between middepth remineralization and the accumulation of recalcitrant carbon, representing a mechanistic analogue to the process of the Microbial Carbon Pump.

To demonstrate this, we have conducted a set of sensitivity experiments comparing simulations with a=0 and a=0.015 under identical physical and biogeochemical forcings. The results show that:

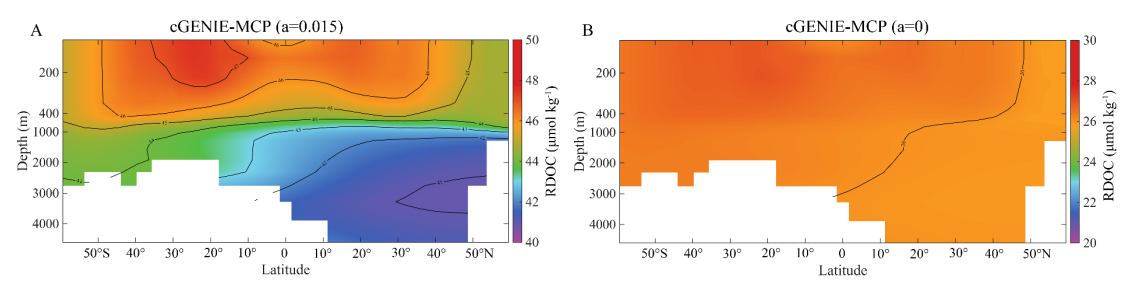
When a=0, the RDOC concentration becomes nearly vertically uniform and its magnitude decreases substantially (see figures below). When a=0.015, by contrast, the model reproduces a more realistic vertical gradient of RDOC.

The concentration pattern reflects the underlying process: when a=0, RDOC behaves as a passive tracer controlled solely by fraction; when a>0, the model resolves an additional slow carbon transfer pathway from SLDOC remineralization, introducing a delayed but continuous source of RDOC. This feedback alters the residence time and vertical redistribution of DOC, generating emergent behavior that cannot be captured by previous unconnected-pool models (e.g., MESMO3).

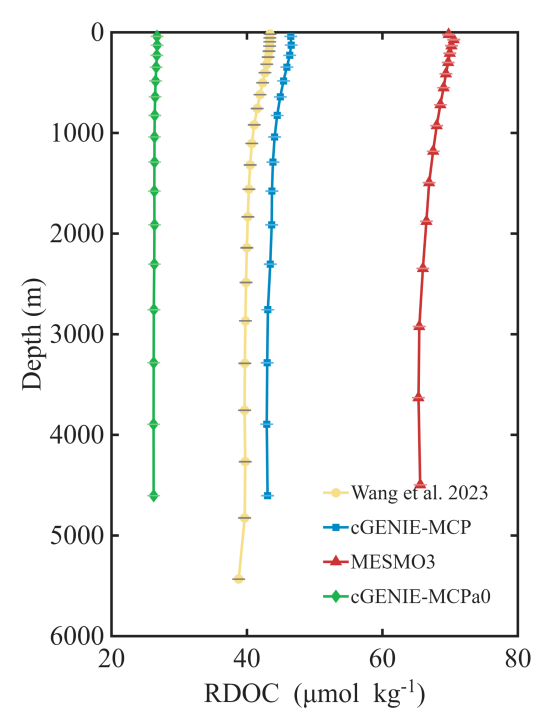
This mechanism is conceptually analogous to the advective-diffusive DOC export identified in recent inverse modeling studies (Wang et al., 2023), where semi-labile DOC contributes to long-term carbon sequestration through slow subduction and remineralization. Therefore, the MCP implementation in cGENIE-MCP represents a mechanistic advance: it links biological production, microbial transformation, and physical transport in a unified framework, allowing the model to simulate long-term DOC dynamics and vertical structures that were not represented in earlier steady-state DOC models.



Surface RDOC concentration (μ mol kg⁻¹). (A) a = 0.015, (B) when a = 0.



DOC concentration (μ mol kg⁻¹) along meridional sections in the central Pacific. (A) a = 0.015, (B) a = 0.



Vertical profiles of RDOC concentration comparing with the results of MESMO3 and Wang et al. (2023). cGENIE-MCP is the result by setting a=0.015, and cGENIE-MCPa0 represents a=0.

Choice of results to evaluate the model

Overall, the results section is heavily weighted towards assessing major ocean tracers not DOC. I understand the authors want to demonstrate their new development doesn't degrade overall model performance but arguably adding a component of organic matter cycling that is characterised by relatively small rates is probably not likely to perturb tracers like PO_4 , O_2 or DIC that much. Table 2 in the manuscript summarises this immediately such that the following text and figures don't add much more highly relevant information. I would suggest minimising this part of the results substantially and/or relocating to supplementary.

It is useful to show temperature as it determines some rates in the model but the only feedback between ocean biogeochemistry and the physical model I'm aware of in cGENIE is atmospheric CO₂, which here is restored to a preindustrial value in these runs. Therefore, temperature does not need evaluating to the extent it is here.

The description should increase its evaluation of DOC in the model since this is the key focus of the new development. The existing evaluation is much briefer and less quantitative for DOC than of other tracers limiting comparison against previous developments and current constraints. Some of this appears in supplementary and would be more informative in the main text. It would be good to see some standard metrics comparable to Table 1 in Hansell (2013) such as inventory (Pg C) production rate (Pg C yr¹), removal rate, lifetime (years) for each of the DOC components. It would also be helpful to see the cGENIE and cGENIE-MCP comparison which is shown

for other tracers but not DOC – is the labile DOC similar between models? It's notable that isotopes are omitted in this manuscript when one of the main advantages of cGENIE is its ability to resolve isotopes! The bulk radiocarbon age is a key constraint on DOC cycling which could be added to the evaluation.

Response:

We have carefully revised the Results section to address these concerns as follows:

1. Rebalancing the focus of the Results section:

We agree that the evaluation of PO₄, O₂, and DIC in the original version was too extensive relative to the DOC assessment. In the revised manuscript, these analyses have been substantially shortened and relocated to the Supplementary Information (Figures S1-S7). The main text now focuses on DOC and its components, highlighting the model's new developments and their implications for the global carbon cycle.

2. Temperature evaluation:

We acknowledge that temperature feedback in the cGENIE framework is primarily via atmospheric CO₂, which is restored to preindustrial levels in our experiments. Accordingly, we have reduced the discussion of temperature in the main text and now only include it briefly to illustrate its role in controlling key biogeochemical rate processes. In the revised manuscript, the relevant section now reads as (Lines 271-289):

"Ocean surface temperature plays a crucial role in biogeochemical cycling and nutrient uptake (Yan et al., 2024). To assess the performance of the cGENIE-MCP model, simulated temperature, PO₄, O₂, and DIC fields were evaluated against observations from the WOA23 and GLODAP at three representative depth levels: surface, intermediate (400 m), and deep (3000 m) layers. As shown in Fig. 3, the cGENIE-MCP model reproduces the large-scale spatial distribution of ocean temperature, capturing major patterns in the surface and low-latitude regions. Temperature decreases from the tropics to the poles and shows little variability in the deep ocean (Fig. 4). The model agrees well with observations, with regional RMSEs of 0.6-1.2 °C (Table 2). Minor biases occur in high-latitude, deep, and upwelling regions, likely due to simplifications in the atmospheric component and limited upper-ocean stratification.

The cGENIE-MCP model also effectively reproduces the large-scale spatial and vertical distributions of PO₄, O₂, DIC, and alkalinity compared with WOA23 and GLODAP datasets (Table 2 and Fig. S1-S7). Modeled PO₄ concentrations (0-4.5 μmol kg⁻¹) and vertical profiles closely match observations, with an overall RMSE of ~0.1 μmol kg⁻¹ (Fig. S1-S2). Simulated dissolved oxygen (DO) patterns align well with observed gradients and OMZ structures, yielding an RMSE of 50-52 μmol kg⁻¹ (Fig. S3-S4). The model slightly underestimates surface DIC and alkalinity due to the use of pre-industrial CO₂ forcing, though accuracy improves under modern CO₂ levels (Fig. S5-S7). Differences between the standard cGENIE and cGENIE-MCP versions are negligible, confirming that inclusion of the RDOM module does not affect the model's physical performance. Overall, the simulated large-scale distributions of PO₄, O₂, and

- 3. Expanded DOC evaluation and quantitative assessment:
- The DOC evaluation section has been expanded considerably. We now include:
- Detailed comparisons between modeled DOC components (LDOC, SLDOC, RDOC) and observations.
- Quantitative model performance metrics, including RMSE values and Taylor diagrams, to assess the agreement between the model and observations (Fig. 10 and Fig. S13).
- Comparisons of DOC and RDOC distributions between cGENIE-MCP and MESMO3 simulations, highlighting differences in the representation of the MCP processes (Fig. 10 and Tab. 3).

Table 3. RMSE of modeled DOC for cGENIE-MCP and MESMO3 compared to observational data

Т	cGENI	E-MCP	MESMO3		
Tracers -	CRMSE	RMSE_vw	CRMSE	RMSE_vw	
Atlantic DOC (μmol kg ⁻¹)	3.63	4.48	12.38	29.47	
Pacific DOC (µmol kg ⁻¹)	3.84	5.34	14.62	31.05	
Indian DOC (μmol kg ⁻¹)	2.56	4.16	17.01	32.20	

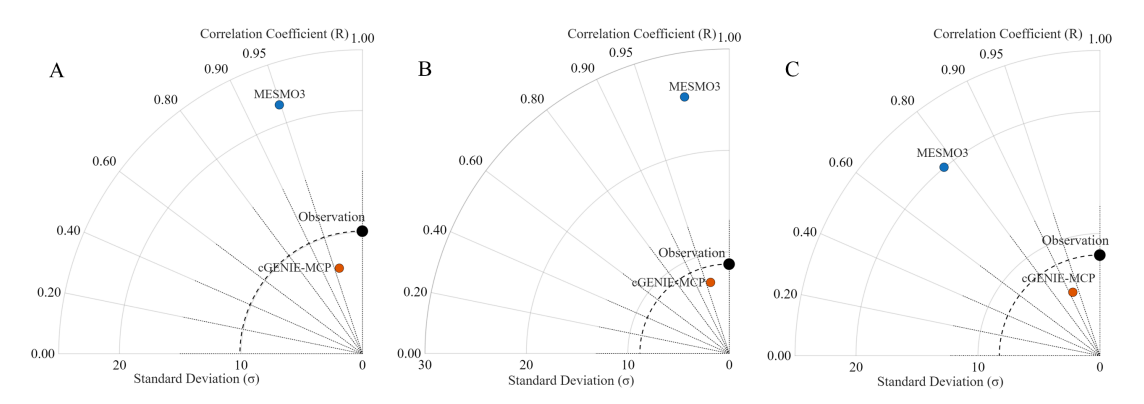


Figure 10. Taylor diagrams comparing simulated DOC concentration from cGENIE-MCP and MESMO3 against observed values from Hansell's laboratory (https://hansell-lab.earth.miami.edu/research/data-collection/) for (A) Atlantic, (B) Indian, and (C) Pacific.

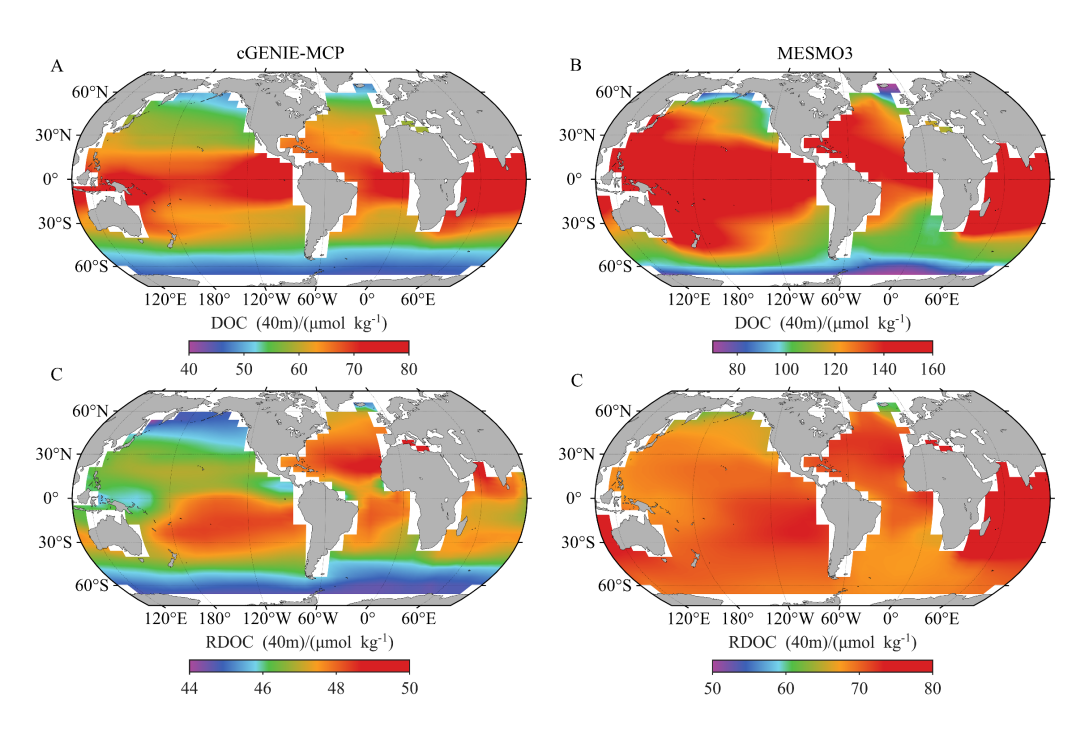


Figure S13. Global distributions of surface (A-B) DOC, (C-D) RDOC concentration (μmol kg⁻¹), (A,C) the results of cGENIE-MCP, (B,D) the results of MESMO3.

And add the following content to the main text (Lines 442-509):

"The statistical evaluation shows that cGENIE-MCP achieves substantial and consistent improvements in simulating DOC concentration compared with MESMO3 across all major ocean basins (Table 3). The cGENIE-MCP yields low CRMSE in the Atlantic (3.63 µmol kg⁻¹), Pacific (3.84 µmol kg⁻¹), Indian (2.56 µmol kg⁻¹) Oceans, whereas MESMO3 exhibits larger values (Atlantic 12.38, Pacific 14.62, Indian 17.01 μmol kg⁻¹). These results indicate that cGENIE-MCP more accurately captures the spatial variability of DOC, while MESMO3 exhibits larger deviations from observed distributions. When errors are weighted by model grid cell volumes (RMSE vw), the contrast between the two models becomes even more pronounced. The cGENIE-MCP maintains relatively low RMSE vw values of 4-5 µmol kg⁻¹, while MESMO3 exhibits much larger errors of ~29-32 μmol kg⁻¹ across all basins, suggesting the DOC bias in MESMO3 exist throughout the water column, particularly in high-volume regions of the deep ocean. Among all basins, the Indian Ocean shows the best performance for cGENIE-MCP, characterized by the lowest CRMSE and RMSE vw values, possibly reflecting the model's enhanced representation of low-latitude processes. Taylor diagrams shows the bias of modeled DOC from the MESMO3 and cGENIE-MCP models with observations (Figure 10). cGENIE-MCP exhibits a relatively high correlation coefficient and a smaller standard deviation comparable to the observed value in the Atlantic, Pacific and Indian Oceans.

The cGENIE-MCP model reproduces the observed DOC concentration range of approximately 50-80 µmol kg⁻¹ and RDOC of 45-50 µmol kg⁻¹, exhibiting a realistic spatial structure with higher values in low-latitude regions and gradual decreases toward the high latitudes (Fig. 5). In contrast, MESMO3 shows expanded higher

concentrations (DOC: 80-160 µmol kg⁻¹; RDOC: 50-80 µmol kg⁻¹) in mid and low latitudes (Fig. S13). The lack of parameter optimization in MESMO3 may partly explain this bias, as its DOC-related parameters were originally tuned only in their earlier carbon cycling framework (Matsumoto et al., 2020) and lack an explicit representation of the transformation between semi-labile and refractory DOC pools.

By introducing the parameterization that explicitly describes the transformation from SLDOC to RDOC, cGENIE-MCP achieves a more balanced partitioning of DOC components and a more realistic steady-state inventory. The improved agreement with observed DOC distributions indicates that the MCP framework enhances the model's representation of the MCP process and the long-term vertical retention of organic carbon. Furthermore, the cGENIE-MCP reflects a more efficient coupling between production and remineralization processes, preventing excessive accumulation. Overall, cGENIE-MCP captures both the magnitude and spatial gradients of marine DOC more faithfully, providing a more robust tool for evaluating long-term ocean carbon storage and microbial carbon pump dynamics."

4. Comparison with the standard cGENIE model:

A direct DOC comparison with the standard cGENIE model was not included because the standard configuration does not explicitly represent the RDOC tracer or the transformation between DOC components.

5. Metrics from Hansell (2013):

In the revised manuscript, we have now included a detailed comparison of DOC metrics—including inventory (Pg C), production rate (Pg C yr⁻¹), removal rate (µmol C kg⁻¹ yr⁻¹), and lifetime (years)—following the framework of Hansell (2013); Hansell et al. (2009). These results are presented in **Tables 4-6**, which summarize the modeled global budgets of LDOC, SLDOC, and RDOC, and their comparison with observational estimates. This addition allows a more quantitative evaluation of DOC cycling in the model. The results show that the model captures the overall magnitude and vertical partitioning of DOC inventories reasonably well, with surface and intermediate inventories comparable to observations, while the deep RDOC pool is somewhat overestimated. The associated production and removal rates, as well as implied lifetimes, are within the range reported by Hansell (2013) and other studies.

The specific modifications are as follows (Lines 463-481):

"In addition, the fraction of LDOC, SLDOC, and RDOC to total DOC across different water layers is consistent with previous observational estimates (Table 4). In the northwest (NW) Pacific surface layer (<200 m), LDOC and SLDOC account for 5-20% and 15-30% of DOC, respectively, broadly consistent with the ranges reported by Ge et al. (2022). In the deep layer (>1000 m), RDOC dominates (>90%), reflecting its remarkable stability and long residence time in the deep ocean. These comparisons indicate that the model realistically reproduces the vertical partitioning of DOC components. Table 5 provides a comparison of the production rates, removal rates, and lifetimes of the DOC components between this study and Hansell (2013). The modeled global production rates (LDOC: 26 Pg C yr⁻¹; SLDOC: 3.9 Pg C yr⁻¹; RDOC: 0.06 Pg

C yr⁻¹) align closely with literature values, further validating the model's parameterization of organic carbon transformation and export. The removal rates of LDOC and SLDOC show approximately 133 and 5 μmol C kg⁻¹ yr⁻¹, respectively, consistent with literature estimates and reflecting the turnover of fast- and intermediate-cycling DOC pools. The RDOC pool exhibits a much slower removal rate (~0.015 μmol C kg⁻¹ yr⁻¹), capturing the long-lived characteristics of RDOC in the deep ocean. Table 6 presents the modeled global DOC inventories across different depths compared with the estimates of Hansell et al. (2009). The model reproduces the surface and intermediate-depth DOC inventories (0-1000 m) reasonably well (0-200 m: 49.8 vs 47 PgC; 200-1000 m: 166.8 vs 185 PgC), but shows a higher inventory in the deep ocean (553.99 PgC vs. 477 PgC), leading to a higher total global DOC inventory. Overall, the combined evidence from Tables 4-6 indicates that the cGENIE-MCP model realistically simulates both the size and total and vertical partitioning of total and component DOC pools."

Table 4 The LDOC, SLDOC, and RDOC percentages from previous studies

Study Region	Water Layer	LDOC	SLDOC	RDOC	Reference
NW	Surface < 200	20-	15-	Deep >1000	Ge et al.
Pacific	m	40%	20%	m: >90%	(2022)
NW	Surface < 200	5 200%	15-30%	Deep >1000 m: >90%	This study
Pacific	m	3-20%	13-30%	m: >90%	This study

Table 5 The production rate, removal rate, lifetime of DOC pools in the model compared with previous studies

Fracti	Production rate (Pg C yr ⁻¹)		Removal rat		Lifetime (years)	
on	Hansell	This	Hansell	This	Hansell	This
	(2013)	study	(2013)	study	(2013)	study
LDO C	15-25	~26	~100	133	~0.001	0.5
SLDO C	~3.74	~3.9	~0.2-9	5	~1.5-20	5
RDO C	~0.04	~0.06	~0.003	0.015	~16000	16000

Table 6 The global inventories of LDOC, SLDOC, and RDOC in the model compared with previous studies

	Inventory (PgC)				
Depth Zone	LDO C	SLDOC	RDOC	DOC	Hansell et al. (2009)-DOC
0-200 m	1.32	8.8	39.67	49.79	47
200-1000 m	0.02	4.42	162.34	166.78	185

>1000 m	0	0.27	553.72	553.99	477
0-bottom	1.34	13.49	755.73	770.56	662

In addition, a spatial distribution of the removal rate has been added, and the following description has been included in the revised manuscript (Lines 427-440):

"The DOC removal rate exhibits pronounced latitudinal gradients, with maxima exceeding 1000-1500 mmol m⁻² yr⁻¹ in the subtropical gyres and North Atlantic meridional overturning regions (Fig. 9A). LDOC removal rate reaches up to 1500 mmol m⁻² yr⁻¹ in the equatorial subtropical gyres and Southern Ocean. SLDOC removal occurs at moderate rates (100-400 mmol m⁻² yr⁻¹), broadly following the spatial patterns of LDOC but extending further into subtropical gyres, indicating its slower turnover. In contrast, RDOC removal remains extremely low (<15 mmol m⁻² yr⁻¹) and spatially uniform, highlighting its resistance to microbial degradation and its long residence time in the ocean interior. These patterns reflect the hierarchy of DOC reactivity (LDOC>SLDOC>RDOC) and emphasize the progressive stabilization of organic carbon as it transitions from labile to refractory pools, underscoring the key role of RDOC in long-term carbon sequestration."

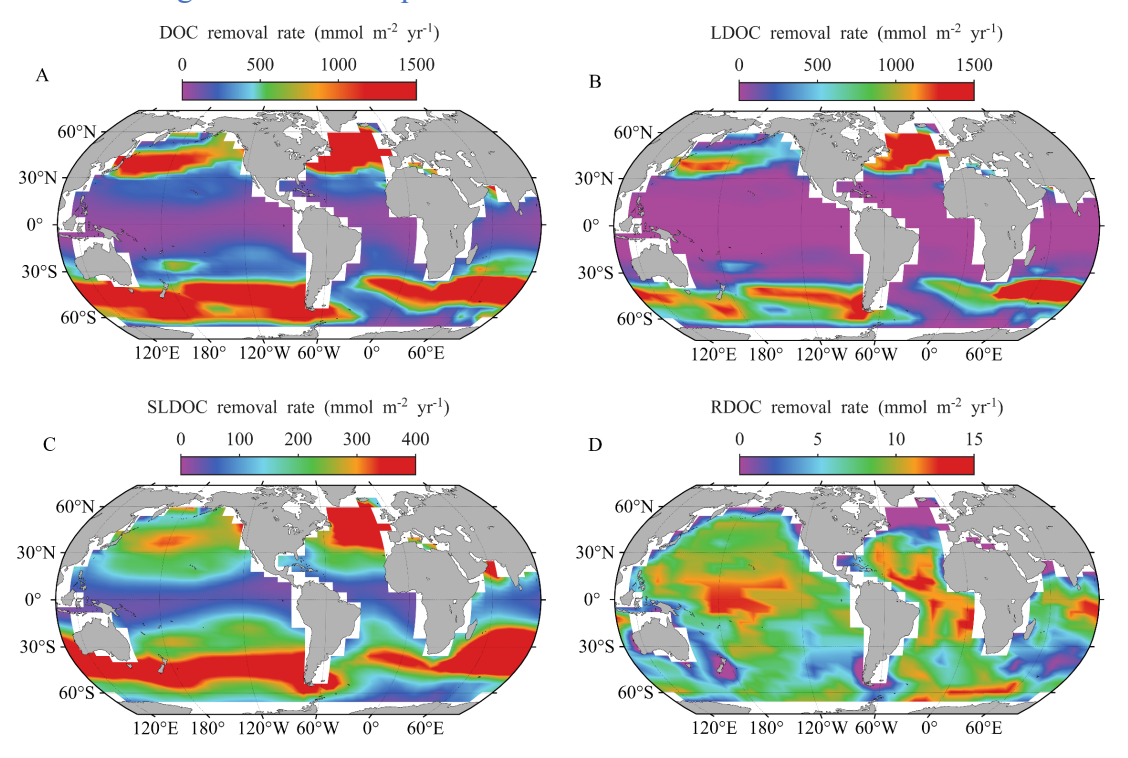


Figure 9. Water column (>130 m) integrated rates of removal for (A) DOC, (B)LDOC, (C)SLDOC, (D)RDOC (mmol m⁻² yr⁻¹), respectively.

6. On isotopic tracers and radiocarbon age:

We fully agree that the inclusion of DOC isotopic evaluation would strengthen the study. However, the current work focuses on developing and validating the DOC cycling framework within cGENIE-MCP, and isotopic tracers were not activated in these simulations. We incorporated the DOC δ^{13} C and Δ^{14} C diagnostics in our model and the

Functionality of the model Several things make the model less functional or harder to use from the description:

a) The tracer names are misaligned between the manuscript and model (LDOC = DOC; SLDOC = RDOC, RDOC = URDOC in the manuscript and model respectively). Ideally, these should be the same.

Response:

We agree that the naming of DOC tracers in manuscript we defined should be the same the code. However, the standard cGENIE used RDOC which is actually the behavior of SLDOC. The renaming in the code has some risks to blow up the result. Therefore, we decide to keep the original name. We added a table in the Supplementary Information (**Table S2**) to clarify this point.

Table S2. Mapping of tracer names between the cGENIE-MCP model code and the manuscript.

Model tracer name	Manuscript name	Description			
DOC	LDOC	Labile dissolved organic carbon			
RDOC	SLDOC	Semi-labile dissolved organic carbon			
URDOC	RDOC	Refractory dissolved organic carbon			

b) Some MCP parameters are hard-coded (f1, f2, a) which reduces the ability of users to explore the MCP. In your discussion you discuss being able to explore the dynamics of the MCP in detail with this model but not being able to change these parameters is a very big limitation to this.

Response:

We thank the reviewer for raising this important point. We agree that, given some MCP parameters (f1, f2, a) are currently hard-coded, the ability to fully explore MCP dynamics is limited in the present implementation. To address this, we have revised the sentence at Lines 519-520 to more accurately reflect what the model can achieve. The revised sentence now reads: "The cGENIE-MCP model proposed in this study can simulate the DOC distribution over geological periods and explore the relationship between DOC response and long-term climate change." This revised wording avoids implying that the current model can flexibly explore the MCP parameter space. In addition, we have added a clarification in Lines 556-560: "Nevertheless, the current implementation relies on hard-coded MCP parameters (f1, f2, a), which constrain the exploration of the MCP dynamics. Future developments will address this limitation by externalizing these parameters in the configuration files, thereby enabling systematic sensitivity analyses and enhancing the model's flexibility and applicability."

c) The activation energy of LDOC is hard-coded to the labile POC parameter so there is no ability to decouple these. Is it reasonable to assume POC and LDOC will be always treated the same?

Response:

In the current model configuration, the temperature dependence of LDOC remineralization is indeed linked to that of the labile POC fraction, following the hard-coded parameterization inherited from cGENIE. This implies that the activation energy for LDOC is not independently adjustable, and the model assumes that LDOC and labile POC respond similarly to temperature. We acknowledge that this is a simplification and may not fully capture potential differences in biochemical composition and reactivity between LDOC and POC. In future work, we plan to implement a decoupled treatment, allowing LDOC to have its own activation energy and temperature-dependent remineralization rate. This would enable a more flexible representation of DOM dynamics and could improve model fidelity in regions where LDOC behaves differently from POC.

Evaluation and presentation

a) The projection choice for Figure 2 limits comparison against other figures. It has no longitude or latitude values.

Response:

While we retained the original projection in Figure 2, because this projection can better emphasize the large-scale distribution of the major ocean basins, we have revised the figure by adding latitude and longitude gridlines as well as regional labels.

The modified diagram is as follows:

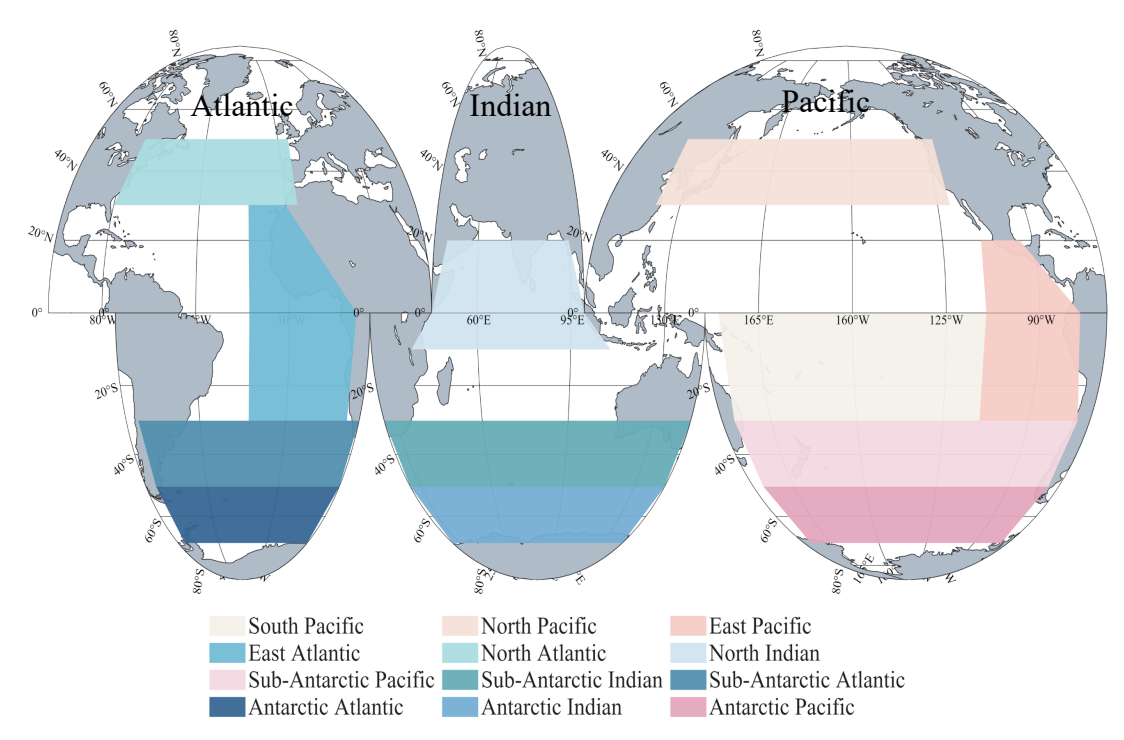


Figure 2. Ocean regions used for model validation in the cGENIE-MCP simulations. Colored regions indicate the spatial domains included in the validation of water column biogeochemical properties. Unshaded areas are excluded from the analysis due to limited relevance or observational data availability.

b) The RMSE presented is actually the centered-RMSE which is the underlying statistic for the Taylor diagram (Jolliff et al., 2009). It would be more informative to show a Taylor diagram so we can assess the spatial distribution and variability of tracers between the two model versions.

Response:

We acknowledge that the previously presented RMSE corresponds to the centered RMSE (CRMSD), which is the statistic underlying Taylor diagrams. In the revised manuscript, we have added the global volume-weighted RMSE (**Table 2 and Table 3**) to provide the absolute error magnitude, and **a Taylor diagram has been included** (Fig. 9) to better illustrate the spatial distribution and variability between the model versions. This allows a more comprehensive evaluation of model performance.

c) Please also consider other misfit functions to assess the model Kriest et al., (2010) provides a good overview of approaches as well as the impact of volume weighting. This discussion may be relevant here because DOC is considerably more variable in the upper ocean than the deep ocean which these alternative functions can deal with.

Response:

In addition to the centered-RMSE used in the Taylor diagram, we have now included

the volume-weighted RMSE and normalized mean bias to better account for the vertical heterogeneity of DOC distributions. As DOC exhibits much greater variability in the upper ocean, volume weighting provides a more balanced evaluation of model skill. The results of these additional metrics have been incorporated into the revised manuscript (see Section 3.1 and Section 3.1, Table 2 and Table 3), and discussed in the context of surface versus deep-ocean variability.

The revised manuscript now explicitly defines RMSE vw as:

$$RMSE_{vw} = \sqrt{\frac{\sum_{i=1}^{N} V_{i} (X_{i} - Y_{i})^{2}}{\sum_{i=1}^{N} V_{i}}},$$

Where V_i represents the actual grid cell volume at position i, computed from the corresponding grid cell surface area and layer thickness ($V_i = A_i \times \Delta Z_i$), A_i represents the horizontal area, ΔZ_i represents the vertical thickness. The CRMSE and correlation coefficient were used to construct the Taylor diagram (Taylor, 2001), providing an assessment of the spatial pattern similarity between models and observations. In addition, the RMSE_vw was calculated to quantify the overall magnitude of model-data deviations by accounting for the oceanic grid-cell volume. While CRMSE emphasizes pattern agreement, RMSE_vw highlights the absolute error in a physically weighted sense, thus offering complementary insights.

d) Why are there no quantitative analysis of the DOC comparison, e.g., RMSE?

Response:

We have now included a quantitative evaluation of the model-data comparison by calculating the root mean square error (RMSE) between the simulated and observed DOC concentrations. The RMSE values for each region are now presented in Section 3.5 Table 3.

e) What is the reason for using specific regions for the model-data comparison? These have been changed from those used in Crichton et al. (2021) with no justification beyond "limited relevance or observational data availability" (Lines 251-252). What does this mean and what is the basis for choosing these regions?

Response:

We have clarified the rationale for redefining the comparison regions in the revised manuscript. Compared to Crichton et al. (2021), the regional division was refined from 8 to 12 regions to better capture basin-scale differences in oceanographic conditions and biogeochemical gradients, and to align with the spatial coverage of available observational data. In particular, the Southern Ocean is subdivided into sub-Antarctic and Antarctic sectors for each basin (Pacific, Indian, Atlantic) to represent distinct water mass characteristics and particle flux regimes. This refinement ensures that each region used for model-data comparison is both coherent in oceanographic properties and

sufficiently supported by observations. These changes are now described in the manuscript (see Lines 257-262 and Figure 2)

f) What do the error bars represent in the vertical profiles?

Response:

The error bars shown in the vertical profiles correspond to the standard deviation (1σ) of the variable across all grid cells within the selected latitude–longitude range at each depth level.

g) The model description does not clearly distinguish between new developments to cGENIE and previous developments. I would suggest to minimise descriptions of existing processes such as air-sea gas exchange, unless they provide important context, to avoid assumptions that they are included in the new developments of cGENIE.

Response:

In the revised manuscript, we have streamlined the model description to focus on the processes directly relevant to this study. Specifically, the description of air-sea gas exchange has been moved to the Supporting Information. The main text now only retains descriptions of the biological production and remineralization processes, which are central to the new developments introduced in this study.

h) There are numerous descriptions of the model fit to observations throughout that aren't supported quantitatively, e.g., "good accuracy" "show good agreement" "more accurately" "moderate discrepancies" "approximately reasonable". This language should be modified unless it is directly related to a quantitative measure.

Response:

We have revised the manuscript to avoid qualitative terms such as "good accuracy", "more accurately", and "approximately reasonable" that are not directly supported by quantitative measures. All descriptions of model performance now use neutral language such as "captures the general pattern", "generally match observations", or "better represent gradients".

Specific Comments

Line 56: "observed RDOC" - more accurately this should be observed deep-ocean bulk [DOC] as there are competing hypotheses about whether this is labile or a mixture of compounds with different reactivities, e.g., Follett et al., (2014).

Response:

We have replaced "observed RDOC" with "observed deep-ocean bulk DOC" throughout the manuscript and added a sentence explaining that bulk DOC observations represent a mixture of compounds with differing reactivities (Follett et al., 2014). This change avoids implying that observations uniquely identify a refractory pool. (See revised text in Line 56)

Lines 59-60: The deep ocean [DOC] and radiocarbon signature issues can be alleviated by adding a simple RDOC pool without MCP parameterisations. The MCP parameterisations add specific dynamics related to why the RDOC accumulates.

Response:

We have revised the manuscript to explicitly state that adding a simple RDOC pool can mitigate the concentration and Δ^{14} C mismatches, whereas MCP parameterizations introduce mechanisms that explain the origin and stability of RDOC (Lines 59-61): "Introducing a simple RDOC pool can reconcile these discrepancies in both DOC concentration and radiocarbon age; while MCP parameterizations offer mechanistic insights into the processes driving RDOC accumulation."

Lines 78-81: It would be good to explicitly explain how MESMO represents SLDOC and RDOC to enable direct comparison with cGENIE-MCP here.

Response:

We have revised the text (Lines 77-84) to explicitly describe how MESMO3 represents semi-labile and refractory DOM pools. Specifically, we now state: "The Minnesota Earth System Model for Ocean biogeochemistry (MESMO 3), an Earth system model of intermediate complexity derived from cGENIE, includes an explicit treatment of semi-labile and refractory DOM pools. In MESMO3, the remineralization of refractory DOM is represented by three additive sinks: slow background decay, surface photodegradation, and complete removal through hydrothermal vent circulation (Matsumoto et al., 2021). However, MESMO 3 lacks a mechanistic representation of DOM production pathways associated with MCP processes—specifically, the transformation of semi-labile DOC (SLDOC) into RDOC—and has not been calibrated against global DOM observations." This revision enables a more direct comparison with the cGENIE-MCP representation.

Lines 103-104: The physical circulation parameters are derived from Cao et al., (2009) configuration but you are using a different continental grid to them (worlg4 vs worjh2). I think the Ward et al., (2018) citation might be more appropriate.

Response:

We have revised the manuscript to reference Ward et al. (2018) for the worlg4 continental grid used in our experiments.

Lines 119-120: Though some details in that paper are relevant here, Ward et al., (2018) describes the trait-based ecosystem so it might help to clarify this distinction here. Are the parameter values or equations used developed in the Matsumoto or Tanioka papers?

Response:

We have clarified this point in the revised manuscript. Specifically, we now state: "Ward et al. (2018) describes a trait-based ecosystem, which is distinct from the DOC parameterization considered here. In this study, the parameter values and equations are primarily based on Matsumoto et al. (2008) and Crichton et al. (2021)."

Line 121: "particulate organic matters (POMs)" – usually this would just be singular not plural.

Response:

We have corrected "particulate organic matter (POM)" throughout the manuscript. (Line 124)

Line 163: "primary production" – GENIE resolves net export production which is equivalent to net community production (NCP) across large enough spatial scales and temporal scales. Primary production is ambiguous to this difference and should probably be avoided.

Response:

We have replaced ambiguous uses of "primary production" with "net export production". (Line 151)

Line 228: "a is the conversion rate" – this does not have units of a rate

Response:

we corrected the wording. "a" is now described as a conversion coefficient

(dimensionless fraction). (Line 220)

Lines 310 -311: or equally that the addition of RDOC has a negligible effect on the largescale PO₄ distribution?

Response:

We have performed an experiment comparing runs with and without the RDOC pool. The addition of RDOC produces negligible changes in large-scale PO₄ (global mean difference=0.01 µmol kg⁻¹). We have added a comparison in Results and Figs. S1-S2.

Lines 347–350: A more appropriate experiment would be a run forced with historical atmospheric CO₂ concentrations from the preindustrial to present-day continuing from your preindustrial spin-up. Or alternatively compare against the GLODAP DIC observations with the anthropogenic DIC component removed (Cant in GLODAP).

Response:

We conducted an additional transient simulation forced with historical atmospheric CO₂ from 1750 to the present (continuing from the preindustrial spin-up). Results are presented in Fig. S7, showing the modelled anthropogenic DIC and comparison to observations.

Line 371: "DOC is a key component of ocean carbon cycling" – maybe my comment is not exactly relevant to here but this refers to multiple things. The recycling of labile DOC is crucial for models to resolve productivity. RDOC is potentially important for carbon storage though this is subject to the timescale discussed.

Response:

We have revised the sentence in Line 306: "DOC is the key update of this model."

Lines 377-380: "cGENIE-MCP model exhibits improved agreement with observed DOC distributions in both surface and deep layers [compared to MESMO 3]" – please quantify this! Can you get the MESMO-3 results and compare concentrations, distributions, RMSE? Otherwise, this is an unqualified statement that cannot be verified.

Response:

We have conducted a quantitative comparison between the DOC fields simulated by cGENIE-MCP and MESMO3, using the same observational dataset (Hansell et al., 2012). The results are now summarized in Table 3, Figs. 9-10, and discussed in Section

3.3 of the revised manuscript.

Table 3 presents the centered RMSE (CRMSE) and volume-weighted RMSE (RMSE_vw) values for both models across the Atlantic, Pacific, and Indian Oceans. The results demonstrate that cGENIE-MCP substantially reduces DOC biases relative to MESMO3 in all basins. For instance, CRMSE values for cGENIE-MCP are 3.63, 3.84, and 2.56 μmol kg⁻¹ in the Atlantic, Pacific, and Indian Oceans, respectively, considerably lower than MESMO3 corresponding values of 12.38, 14.62, and 17.01 μmol kg⁻¹. Similarly, the RMSE_vw results show a consistent improvement (4-5 μmol kg⁻¹ for cGENIE-MCP vs. 29-32 μmol kg⁻¹ for MESMO3), indicating that the MESMO3 biases are both stronger in magnitude and more pervasive throughout the water column.

The Taylor diagrams (Fig. 10) further confirm that cGENIE-MCP achieves higher pattern correlations (R > 0.9) and smaller normalized standard deviation differences with respect to observations, reflecting an improved representation of spatial variability. Figure 11 shows that the global DOC and RDOC distributions simulated by cGENIE-MCP match the observed ranges (DOC: 50-80 μ mol kg⁻¹; RDOC: 45-50 μ mol kg⁻¹) and reproduce realistic latitudinal gradients, whereas MESMO3 systematically overestimates concentrations (DOC: 80-160 μ mol kg⁻¹; RDOC: 50-80 μ mol kg⁻¹), especially in low-latitude surface waters.

This improvement primarily arises from the MCP parameterization and configuration in cGENIE-MCP, and explicitly couples the semi-labile and refractory DOC pools through the transformation term a×[SLDOC]. This process enhances the balance between DOC production, transformation, and remineralization, thereby reducing excessive DOC accumulation present in MESMO3.

In summary, the newly added quantitative comparisons (Tables 3-4; Fig. 10; Fig. S13) demonstrate that cGENIE-MCP provides a consistent and significant improvement over MESMO3 in reproducing observed DOC magnitudes, vertical gradients, and spatial variability. The statement on improved model performance has been accordingly revised and substantiated with these results in the revised manuscript.

Lines 398-403: The supplementary figures and tables (Fig S6, Tables S2 and S3) need to be in the main text as these are essential comparisons against observations and models of DOC, which is the key focus of this manuscript.

Response:

We have moved Tables S2 and S3 to the main text (now Tables 4 and 5) and expanded the analysis by including quantitative comparisons against MESMO3 and adding a Taylor diagram to illustrate model performance in terms of spatial variability and correlation with observations. These additions strengthen the evaluation of DOC and RDOC simulations and provide a clearer comparison among cGENIE-MCP, the original cGENIE configuration, and MESMO3. We have retained Fig. S12 in the Supplementary Material, as it presents regional vertical profiles (e.g., the western Sargasso Sea and comparisons with Wang et al. (2023) that serve as supporting

examples to complement the global-scale analyses in the main text. The new Tables and Taylor diagram are now presented after the DOC spatial distribution analysis, where the quantitative mode-data and inter-model evaluations naturally follow the description of DOC patterns.

Line 441: "lifetime of months to years" – you have prescribed a fixed lifetime in the model, it is not variable.

Response:

The original wording may have implied variability, which is not the case in our model. We have revised the sentence to explicitly state that SLDOC is assigned a fixed lifetime in the model, after which it is either remineralized or converted into RDOC.

Figure 13: This is an unusual way of plotting meridional distributions which is pretty hard to interpret. It would be much clearer to show zonal averages for each DOC pool such as in Figure 12.

Response:

We appreciate the reviewer's comment and fully understand that zonal mean plots are often clearer for visualizing large-scale DOC distributions. However, Figure 13 (current Fig. 7) was specifically designed to emphasize the meridional variations of different DOC pools, particularly LDOC and SLDOC, which are strongly confined to the surface and exhibit pronounced regional heterogeneity. Averaging zonally (as in Fig. 6) would obscure these surface-concentrated signals and reduce the visibility of the LDOC and SLDOC gradients.

Lines 452-454: "Slight elevated RDOC concentrations ... may reflect entrainment of surface-derived labile semi-labile DOC..." – is it possible to back this out of the model and demonstrate?

Response:

We agree that the model does not explicitly allow us to separate and demonstrate the entrainment of LDOC/SLDOC during deep water formation. To avoid overstating, we have revised the text to clarify that the observed pattern is consistent with this possibility but cannot be directly backed out from the model. The revised sentence: "Slightly elevated RDOC concentrations in high-latitude deep waters are consistent with the possibility of entrainment of surface-derived labile and semi-labile DOC during deep water formation and ventilation, although this mechanism cannot be explicitly isolated from the model."

Lines 454-457: "These results underscore the dynamic role of LDOC and SLDOC" – I don't think this statement is supported because you have only shown a steady-state results. To support this you need to show that the model behaves differently to some perturbations compared to the model without the interactions between DOC pools that underpin the MCP concept.

Response:

We appreciate this insightful comment. Because our current manuscript focuses on steady-state behavior, we have revised the text to avoid asserting a dynamic role.

Section 4.2: This version of GENIE resolves net export production not primary production. It has no representation of some of the processes described here like top-down grazing pressure, bacterial and viral lysis, particle solubilization – the net effect of these processes are parameterised by the Michaelis-Menten uptake scheme you are using. This discussion should be amended to better reflect what the model is actually doing and how it represents the complex reality.

Response:

We agree that the cGENIE-MCP framework does not explicitly resolve ecological processes such as grazing, lysis, or particle solubilization. These processes are implicitly represented in the model through the Michaelis-Menten uptake scheme and the prescribed partitioning of net export production into LDOC, SLDOC, and RDOC pools. We have revised Section 4.2 accordingly to emphasize that the model resolves net export production rather than explicit primary production and that the biological complexity is represented in a parameterized form.

The revised description is as follows:

"Net export production (PP) is driven by the availability of nutrients and light within the euphotic zone, following a Michaelis-Menten uptake scheme in which phytoplankton convert inorganic carbon into organic matter. The spatial distribution of PP reflects abiotic controls such as nutrient upwelling, stratification, and light limitation, with biological complexity-including grazing, microbial recycling, and viral/bacterial lysis-is represented implicitly through parameterization. In the model, the PP process generates DOC in labile, semi-labile, and refractory fractions, whose spatial and temporal variations are influenced by both biological and environmental factors."

Line 518: "huge RDOC" – please quantify this! The DOC inventory is around 700 Pg C whereas the regenerated DIC pool from the Biological Carbon Pump is around 1700 Pg C which undermines this argument. I would argue it is the potential dynamics that are crucial here – how likely, and by how much, could RDOC and regenerated DIC change in response to perturbations or different factors?

Response:

We have revised the text to replace the qualitative term "huge" with a quantitative and more balanced description. Specifically, the revised sentence now reads (Lines 528-533): "The global ocean DOC reservoir is estimated to contain approximately 700 Pg C (Hansell, 2013). Although this accounts for only about 40% of the regenerated DIC reservoir (~1700 Pg C), it nonetheless represents a significant and long-lived carbon pool in the ocean. Its importance lies in its connection to SLDOC through the MCP process, allowing RDOC to vary in response to physical and biogeochemical perturbations. This dynamic behavior underscores the critical role of RDOC in regulating long-term ocean carbon storage and climate feedbacks."

Line 529: "coupled of ocean carbon pump" – it's not clear what this is referring to.

Response:

Our original intention was to emphasize the overall effects of ocean negative carbon emission technologies in relation to ocean carbon cycling processes. To avoid confusion, we have removed the unclear phrase "coupled of ocean carbon pump" and revised the sentence to: "Future the model can be used to assess the potential of ocean negative carbon emission technologies (e.g., ocean alkalinization enhancement) under different climate scenarios. By simulating alternative implementation pathways, the long-term environmental impacts of these technologies can be quantified, enabling a comprehensive evaluation of optimal deployment strategies for sustainable carbon sequestration." This modification clarifies the intended meaning.

Figure S6: Why is the Sargasso Sea singled out here, and is this modelled or observed concentrations? What area does panel B correspond to-global average? Can the comparison against Wang et al., (2023) be expanded?

Response:

The Sargasso Sea is highlighted in Figure S6 (current Fig. S12) because it is one of the best-characterized regions for long-term DOM observations, providing valuable constraints for model-data comparison, particularly for the refractory DOC pool. In Hansell (2013), there is a picture (Fig. 5) of the Sargasso Sea, which indicates the changes in water column concentrations of LDOC, SLDOC, and RDOC. In panel A, modeled concentrations in the Sargasso Sea are shown to evaluate model performance against regional observations. Panel B presents the global mean vertical distribution of modeled DOC for comparison with available large-scale estimates.

Regarding the comparison with Wang et al. (2023), we agree that expanding this comparison would be valuable. However, since DOC has observational data, while the observational data of RDOC is scarce, since Wang et al. (2023) specifically included RDOC simulations in their study, our comparison with their results mainly focuses on

Tables S2 and S3: This is useful but seems like it could easily expanded. Could you add comparison against MESMO here? Are there other datasets and models that could be compared against? Can the analysis be expanded to more regions?

Response:

Following this recommendation, we have included a quantitative comparison between our simulations and the MESMO3 results. Specifically, we computed both the centered-RMSE (CRMSE) and the volume-weighted RMSE (RMSE_vw) to evaluate model performance and added a Taylor diagram to illustrate the spatial distribution and variability of DOC across models. These additions provide a more comprehensive comparison between cGENIE-MCP and MESMO3.

However, to maintain clarity and focus in Tables S2 and S3 (current Tables 4 and 5), we have not expanded these tables to include MESMO3 results. Instead, the new quantitative comparison and Taylor diagram are presented in Figure 10 and Table 3 of the revised manuscript. We believe this approach provides a clearer presentation of model-model and model-observation comparisons without overcrowding the supplementary tables.

Reference

Crichton, K. A., Wilson, J. D., Ridgwell, A., and Pearson, P. N.: Calibration of temperature-dependent ocean microbial processes in the cGENIE. muffin (v0. 9.13) Earth system model, Geoscientific Model Development, 14, 125-149, 2021.

Dunne, J. P., Armstrong, R. A., Gnanadesikan, A., and Sarmiento, J. L.: Empirical and mechanistic models for the particle export ratio, Global Biogeochemical Cycles, 19, 2005.

Follett, C. L., Repeta, D. J., Rothman, D. H., Xu, L., and Santinelli, C.: Hidden cycle of dissolved organic carbon in the deep ocean, Proceedings of the National Academy of Sciences, 111, 16706-16711, 2014.

Ge, T., Luo, C., Ren, P., Zhang, H., Chen, H., Chen, Z., Zhang, J., and Wang, X.: Dissolved organic carbon along a meridional transect in the western north pacific ocean: Distribution, variation and controlling processes, Frontiers in Marine Science, 9, 909148, 2022.

Hansell, D. A.: Recalcitrant dissolved organic carbon fractions, Ann Rev Mar Sci, 5, 421-445, 2013. Hansell, D. A., Carlson, C. A., Repeta, D. J., and Schlitzer, R.: Dissolved organic matter in the ocean: A controversy stimulates new insights, Oceanography, 22, 202-211, 2009.

Matsumoto, K., Rickaby, R., and Tanioka, T.: Carbon export buffering and CO2 drawdown by flexible phytoplankton C: N: P under glacial conditions, Paleoceanography and Paleoclimatology, 35, e2019PA003823, 2020.

Matsumoto, K., Tanioka, T., and Zahn, J.: MESMO 3: Flexible phytoplankton stoichiometry and refractory dissolved organic matter, Geoscientific Model Development, 14, 2265-2288, 2021.

Matsumoto, K., Tokos, K., Price, A., and Cox, S.: GENIE-M: a new and improved GENIE-1 developed in Minnesota, Geoscientific Model Development Discussions, 1, 1-37, 2008.

Ridgwell, A., Hargreaves, J., Edwards, N. R., Annan, J., Lenton, T. M., Marsh, R., Yool, A., and Watson, A.: Marine geochemical data assimilation in an efficient Earth System Model of global biogeochemical cycling, Biogeosciences, 4, 87-104, 2007.

Ridgwell, A. J.: Glacial-interglacial perturbations in the global carbon cycle, Ph. D. thesis, Univ. of East Anglia, 2001.

Wang, W. L., Fu, W., Le Moigne, F. A. C., Letscher, R. T., Liu, Y., Tang, J. M., and Primeau, F. W.: Biological carbon pump estimate based on multidecadal hydrographic data, Nature, 624, 579-585, 2023.

Wanninkhof, R.: Relationship between wind speed and gas exchange over the ocean, Journal of Geophysical Research: Oceans, 97, 7373-7382, 1992.

Ward, B. A., Wilson, J. D., Death, R. M., Monteiro, F. M., Yool, A., and Ridgwell, A.: EcoGEnlE 1.0: plankton ecology in the cGEnlE Earth system model, Geoscientific Model Development, 11, 4241-4267, 2018.

Yan, C., Lu, Y., Yuan, X., Lai, H., Wang, J., Fu, W., Yang, Y., and Li, F.: Simulation of Vertical Water Temperature Distribution in a Megareservoir: Study of the Xiaowan Reservoir Using a Hybrid Artificial Neural Network Modeling Approach, Journal of Hydrologic Engineering, 29, 04024047, 2024.